Electronic Supplementary Information

Modulation in Ru and Cu nanoparticles contents over CuAlPO-5 in synergistic enhancement in the selective reduction and oxidation of biomass-derived furan based alcohols and carbonyls

Abhinav Kumar[a], Rajaram Bal[b], and Rajendra Srivastava[a]*

[a]*Catalysis Research Laboratory*, *Department of Chemistry, Indian Institute of Technology Ropar, Rupnagar-140001, India*

[b]*Nanocatalysis Area Conversion and Catalysis Division, CSIR-Indian Institute of Petroleum, Dehradun-248005, India*

Corresponding author *Email: rajendra@iitrpr.ac.in

*Phone: +91-1881-232064

Experimental section

Chemicals

Aluminium isopropoxide, furfural, 5-hydroxymethylfurfural, and ruthenium chloride were procured from sigma Aldrich Pvt. Ltd., India. Triethylamine, ortho-phosohric, and cupric nitrate were received from Merk India Pvt. Ltd.. Cupric acetate was purchased from Loba Chemie Pvt. Ltd., India. All used solvents were obtained from Merck and Sigma Pvt. Ltd., India. 3-(trimethoxysilyl)propyl]hexadecyldimethylammonium chloride (TPHAC) was synthesized in the laboratory following the reported procedure.[S1]

Synthesis of CuAlPO-5

The copper aluminophosphate (CuAlPO-5) was synthesized by following the reported procedure using the molar gel composition of 0.1 Cu: 0.95 Al_2O_3: 1 P_2O_5: 1.6 triethylamine: 100 H_2O: 0.1 TPHAC.[32] In a typical synthesis method, the aluminium isopropoxide (4.21 g) was dissolved in 10 g of distilled water under vigorous stirring for 3 h at ambient temperature. Then in the next step, phosphoric acid (2.22 g) was added under stirring condition, and stirring was continued for a further 30 min. Then triethylamine (1.60 g) was added drop-wise under stirring conditions. In the next step, 3-(trimethoxysilyl)propyl]hexadecyldimethylammonium chloride (TPHAC (0.5 g dissolved in 4 g distilled water) was added under vigorous stirring. After 30 min of vigorous stirring, copper acetate (0.5 g dissolved in 4 g distilled water) was drop wise added. The formed gel was allowed to stir further for 2 h under ambient conditions. Then, the resultant gel was transferred into a Teflon-lined autoclave and hydrothermally treated at 473 K for 36 h. The obtained precipitated material was filtered, washed with distilled water, and dried at 373 K for 12 h. The obtained dry solid powder was calcined in a muffle furnace in presence of air at 823 K for 5 h.

Material Characterization

All the synthesized materials were characterized by X-Ray diffraction (XRD) in the 2θ range of 5-80° on a RIGAKU Mini-Flex diffractometer with Cu kα (λ = 0.154 nm) radiation. The porosity and surface area of the materials were determined using N_2 adsorption-desorption analysis on a Quantachrome Autosorb IQ2 Chem/BET instrument. All materials were degassed at 473 K for 3 h before starting the analysis. The specific surface area was determined in the relative pressure range of 0.05 to 0.3 using Brunauer-Emmett-

Teller (BET) equation. The distribution of pores was evaluated using the Barrett-Joyner-Halenda (BJH) method from the desorption branch of the adsorption-desorption isotherm. The morphologies of the materials were characterized using field emission scanning electron microscopy (FE-SEM) on a Quanta 200 F, M/s FEI, Netherlands instrument. The nanostructural morphological information was retrieved from a transmission electron microscope (TEM) (M/s JEOL JSM 2100) instrument operating at 200 kV. The distribution of elements and their composition was analyzed by energy-dispersive X-ray spectroscopy (EDX) and TEM mapping. The elemental presence and their oxidation state were investigated by X-Ray photoelectron spectroscopy (XPS) on a Thermofisher Scientific (Nexsa base) instrument. The amounts of Cu and Ru present in the sample were determined from microwave plasma-atomic emission spectroscopy (MP-AES).The ammonia temperature programmed desorption (NH_3-TPD), temperature-programmed reduction (TPR), and temperature-programmed oxidation (TPO) were performed on a Quantachrome CHEMBET^{TM} TPR/TPD Autosorb-IQ instrument, USA using diluted NH_3 (10 % in He), H_2 (5 % in He), and O_2 (5% in He) as the probe gases. In each case, before analysis, samples were degassed under the He flow for 30 min at a temperature ramp of 10 °C/min. For NH_3-TPD the NH_3 gas was flow for 30 min through the sample to insure complete adsorption at ambient temperature. Then the sample was purge with He gas to remove the physically adsorbed NH_3. In the next step temperature was ramped and the desorption of NH_3 was recorded by a TCD detector as a function of temperature. For TPR and TPO measurements, after sample degassing, the H_2 and O_2 consumption was recorded under the continuous gas flow (10 ml/min). The total H_2 and O_2 consumptions were recorded as function of temperature on a TCD detector.

Determination of activation energy (E_a)

To determine the activation energy of the FAL hydrogenation reaction over Cu(9.25%)Ru(0.75%)/CuAlPO-5, reactions were carried out at three different temperatures (333 K, 343 K, and 353 K) (Fig.S4a). The activation energy of HMF oxidation was calculated over Cu(9%)Ru(1%)/CuAlPO-5 at temperatures of 373 K, 393 K, and 413 K (Fig.S6a). Since in both the reactions, solvent and gas (H_2 or O_2) are taken in excess and the catalyst amount was kept constant, therefore, it follows the first-order kinetics (Eq. 1). From the plot of FAL or HMF conversion and time and considering the first-order kinetics, a plot of –ln (1-x) *vs* time (t) is plotted at three different temperatures (Fig. S4b, Fig. S6b). Slopes

of this plot provide the rate constants of these reactions at three different temperatures. Finally, a plot of ln k vs 1/T is plotted to obtain the activation energy for both the reactions by following equation 2 (Fig. S4c, Fig. S6c). From the slope of the plot, the calculated values of activation energy (E_a) for FAL to FOL hydrogenation and HMF to DFF oxidation are 21.53 and 34.57 kJ/mol, respectively.

$$-\frac{d[FAL\ or\ HMF]}{dt} = k[FAL] = \frac{d[FOL\ or\ DFF]}{dt} \quad (1)$$

$$-\ln(1-x) = kt + c$$

$$lnk = -\left(\frac{E_a}{RT}\right) + lnA \quad (2)$$

Catalyst recyclability and hot-filtration test

The stability and recyclability of catalyst for both FAL reduction and HMF oxidation were carried out using catalysts Cu(9.25%)Ru(0.75%)/CuAlPO-5 and Cu(9%)Ru(1%)/CuAlPO-5, respectively (Fig. S7). After completion of both the reactions,the catalyst was separated by centrifugation, washed with acetone and water, and reused in the next catalytic cycle. After five catalytic cycles, conversion and selectivity were remained constant for both the reactions (Fig. S7 a & b). A hot-filtration test was performed to verify the stability of the catalyst during the reaction. In FAL hydrogenation and HMF oxidation reactions, catalystswere removed from the reaction mixture after 3 and 12 h, respectively. No significant increase in reactant conversion was observed after the removal of the catalyst (Fig.S7 c & d). This confirms that the reaction is purely heterogeneous in nature and no active species was leached during the occurrence of both the reactions, which could catalyze the reaction after removal of the catalyst. The recycled catalyst was characterized by XRD (Fig. S8). The XRD of the spent catalysts were similar to the fresh catalysts. This suggests that both the catalysts were stable during the reactions and they can be used for multiple cycles.

Table S1. The comparative activation energy(E_a) for FAL to FOL transformation.

E. no.	Catalyst	E_a (kJ/mol)	Reference
1.	$Ru_{1.0}Mo_{1.0}P$	51	S2
2.	Ru/ZrO_2	56.0	S3
3.	Au/Al_2O_3	45.0	S4
4.	Pt/C	28	S5
5.	$CuCrO_2$	46.0	S6
6.	Cu/SiO_2	50.2	S7
7.	Cu-Co@SBA-15	38.5	S8
8.	BDT-Pd/Al_2O_3	12 ± 5	S9
9.	$Pd/CuFe_2O_4$	19.7	25
10.	**Cu(9.25%)Ru(0.75%)/CuAlPO-5**	**21.5**	**This study**

Table S2. The comparative activation energy (E_a) for HMF oxidation to DFF.

E. no.	Catalyst	E_a (kJ/mol)	Reference
1.	Cs/MnO_x	58.0	S10
2.	VO_x/TiO_2	67.0 – 77.0	S11, S12
3.	OMS-2	81.0	S13
4.	TEMPO	61.5	S14
5.	Ru(3%)/H-Beta	62.6	60
6.	$Mn\text{-}Co_3O_4$	24.2	S15
7.	**Cu(9%)Ru(1%)/CuAlPO-5**	**34.57**	**This study**

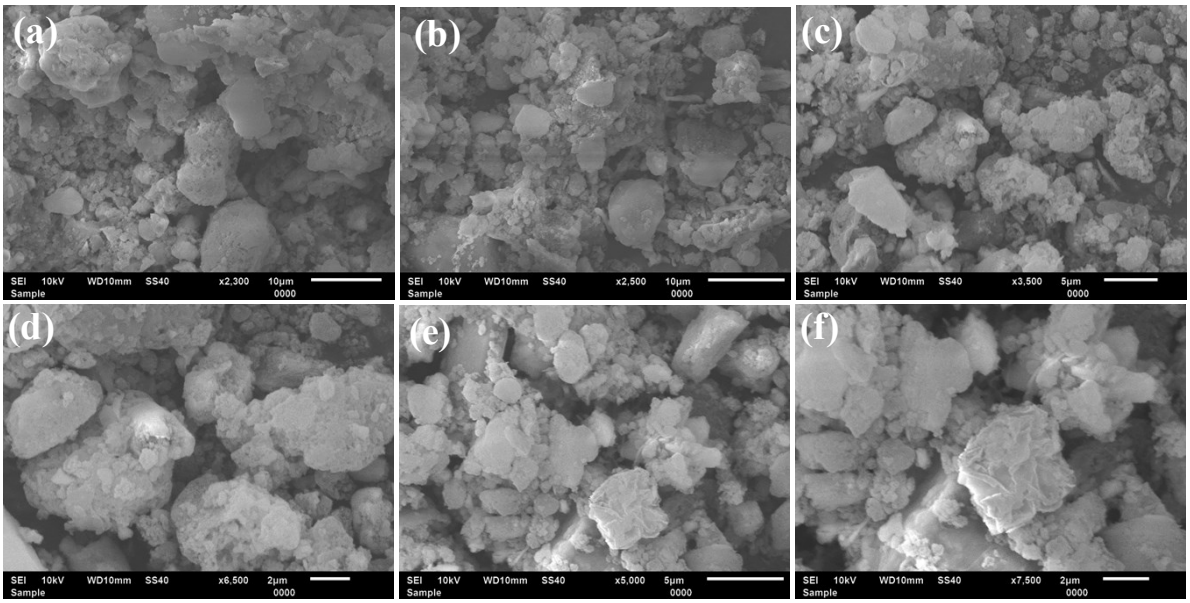

Fig. S1. FE-SEM images of (a,b) CuAlPO-5, (c, d) Cu(9%)Ru(1%)/CuAlPO-5, and (e, f) Cu(9.25%)Ru(0.75%)/CuAlPO-5.

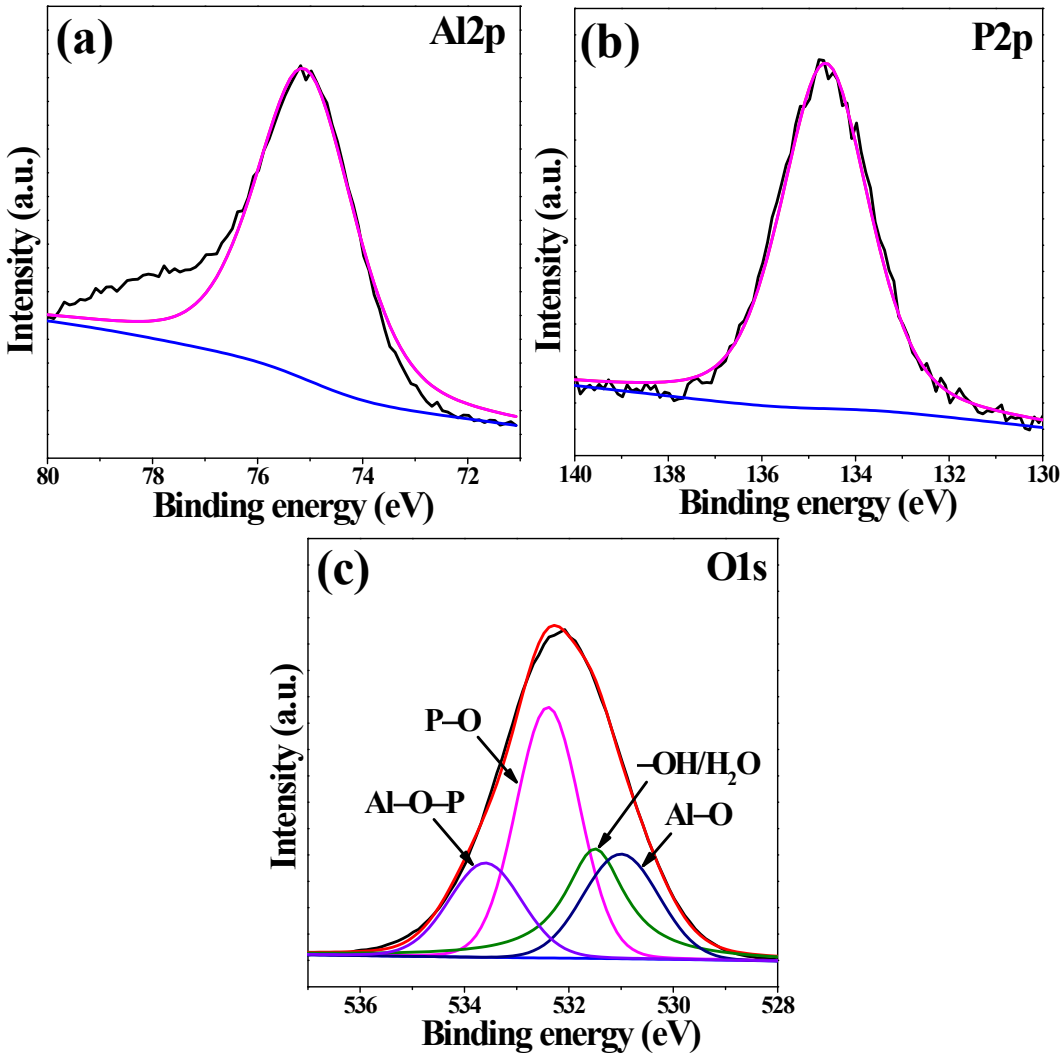

Fig. S2. High resolution spectrum of (a) Al 2p, (b) P 2p, and (c) O 1s.

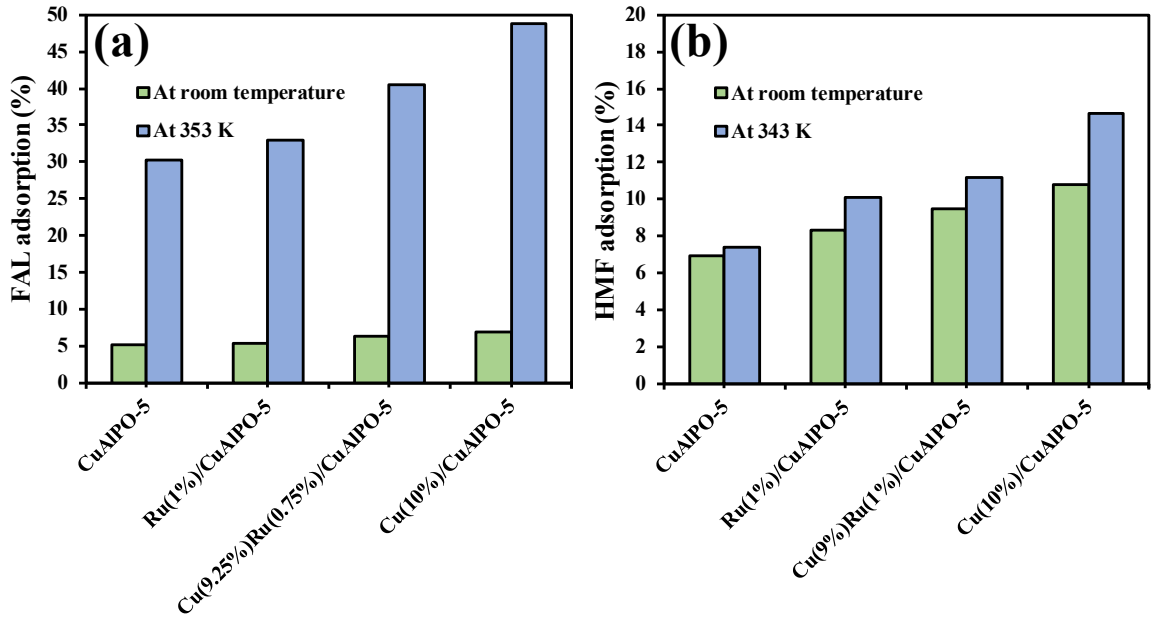

Fig. S3. Adsorption of (a) furfural and (b) HMF over CuAlPO-5, Ru(1%)/CuAlPO-5, Cu(9.25%)Ru(0.75%)/CuAlPO-5, and Cu(10%)/CuAlPO-5.

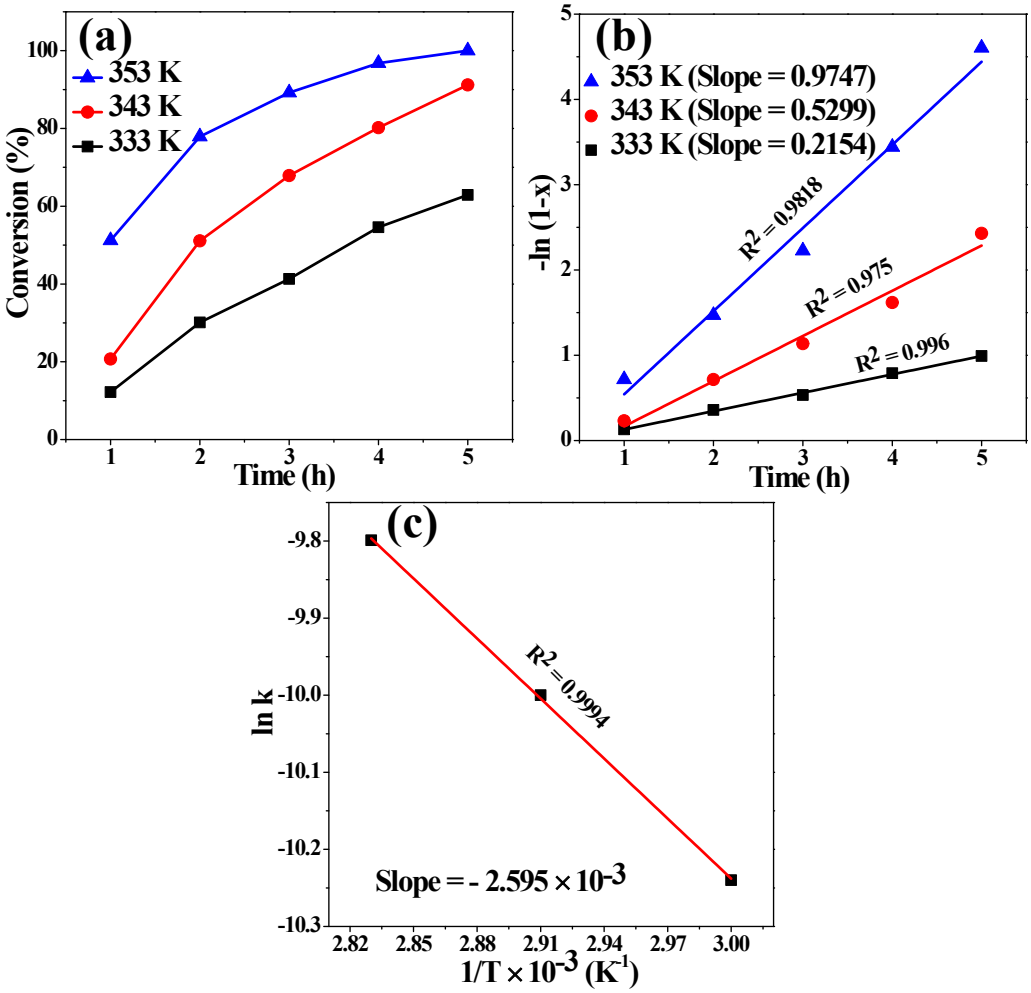

Fig. S4. Kinetic curves for the selective hydrogenation of FAL to FOL (a) relationship between FAL conversion and reaction time, (b) relationship between –ln(1-x) and reaction time, and (c) relationship between ln k and 1/Temperature (1/T). [Reaction condition: furfural (1mmol), Cu(9.25%)Ru(0.75%)/CuAlPO-5 (50 mg), H_2O (10 mL), H_2 (1 MPa).]

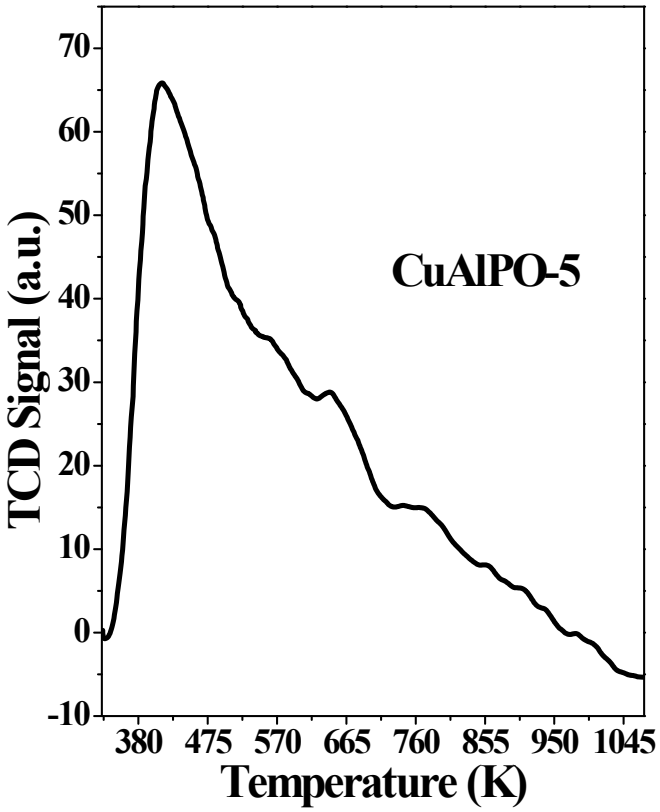

Fig. S5 NH_3-TPD profile of CuAlPO-5.

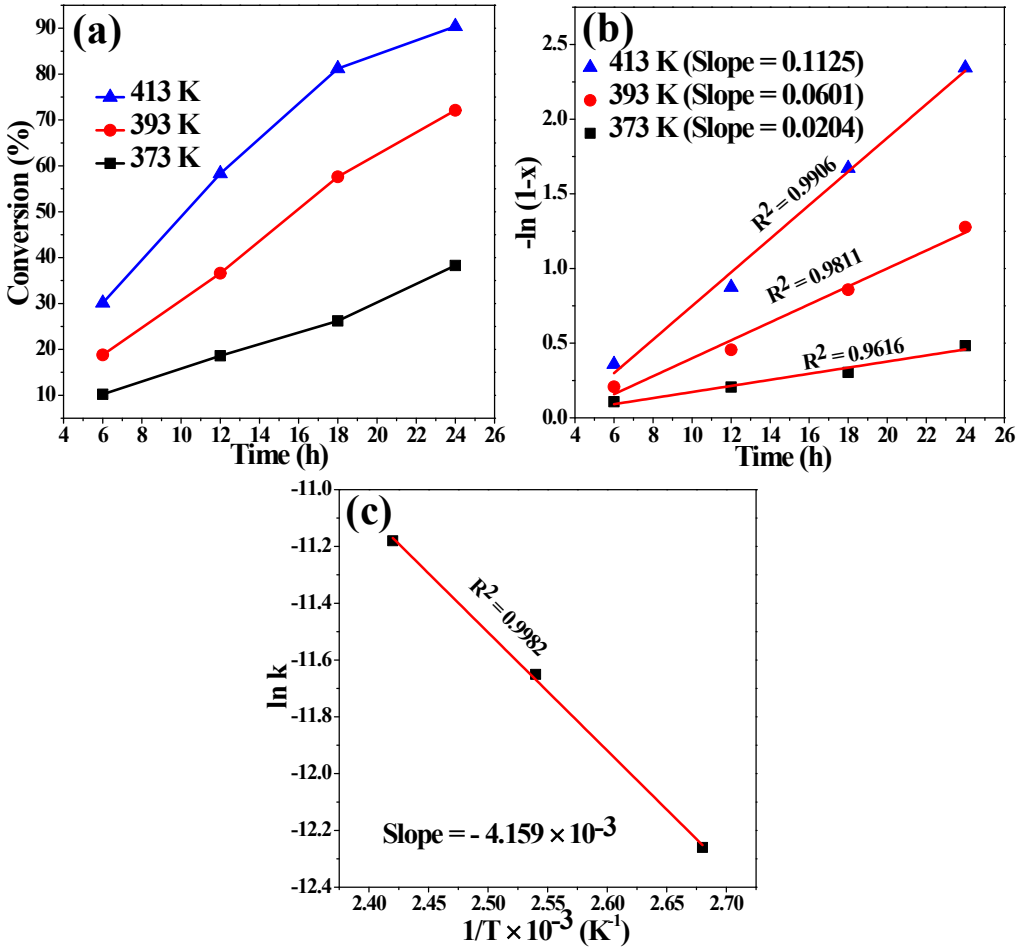

Fig. S6. Kinetic curves for the selective oxidation of HMF to DFF (a) relationship between HMF conversion and reaction time, (b) relationship between –ln(1-x) and reaction time, and (c) relationship between ln k and 1/Temperature (1/T). [Reaction condition: HMF (0.5mmol), Cu(9%)Ru(1%)/CuAlPO-5 (50 mg), DMSO (5 mL), oxygen flow (10 mL/min).]

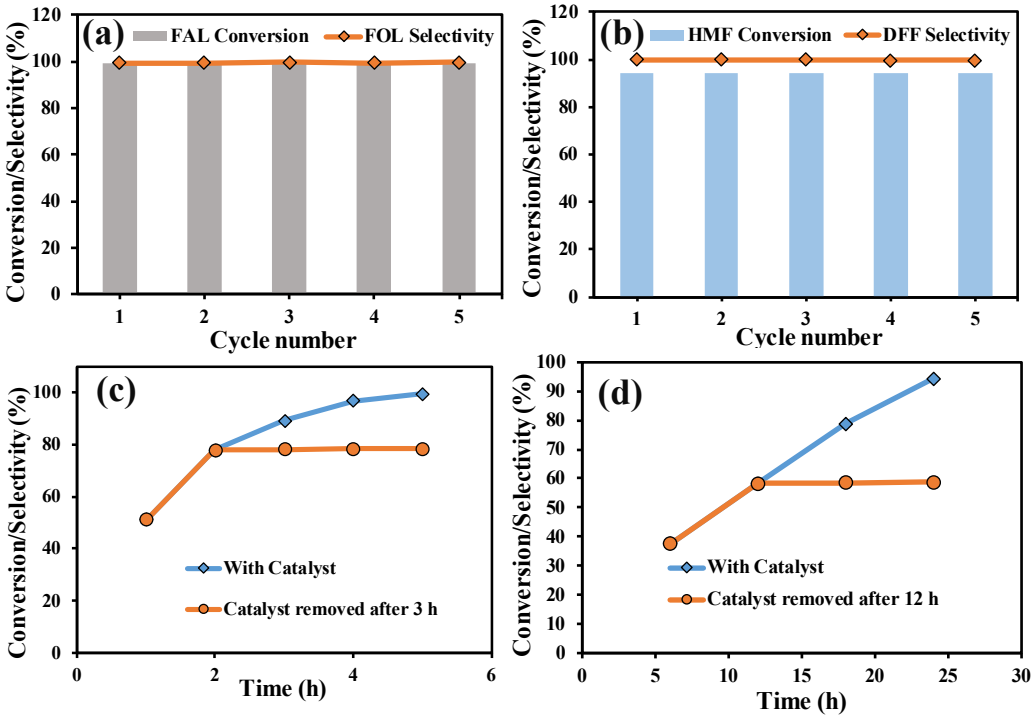

Fig. S7. Catalyst recyclability tests for (a) FAL hydrogenation, (b) HMF oxidation reactions and hot-filtration tests for (c) FAL hydrogenation, (d) HMF oxidation.

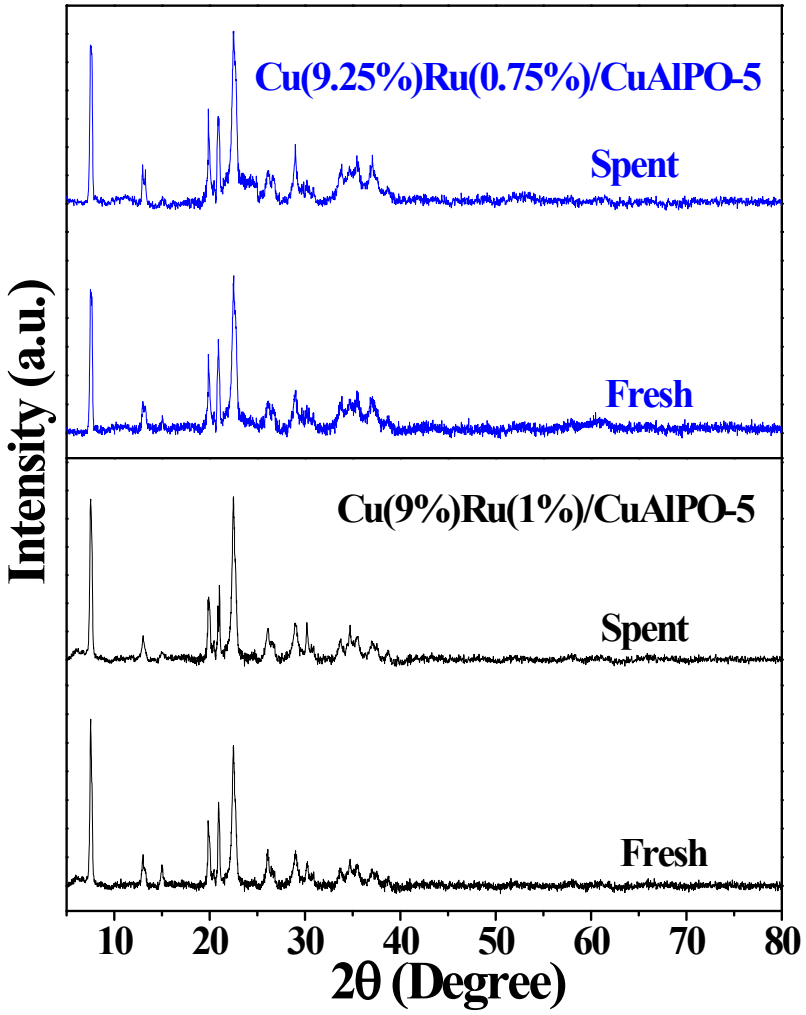

Fig. S8. XRD patterns of fresh and spent catalysts.

Reference

S1 B. Sarmah, R. Srivastava and B. Satpati, *ChemistrySelect*, 2016, **1**, 1047–1056.

S2 Y. Bonita, V. Jain, F. Geng, T.P. Óconnell, W. N. Wilson, N. Rai and J.C. Hicks, *Catal. Sci. Technol.*, 2019, **9**, 3656–3668.

S3 R. Huang, Q. Cui, Q. Yuan, H. Wu, Y. Guan and P. Wu, *ACS Sustain. Chem. Eng.*, 2018, **6**, 6957–6964.

S4 M. Li, Y. Hao, F. Cárdenas-Lizana and M.A. Keane, *Catal. Commun.*, 2015, **69**, 119–122.

S5 P. D. Vaidya and V. V. Mahajani, *Ind. Eng. Chem. Res.*, 2003, **42**, 3881–3885.

S6 R. Rao, A. Dandekar, R.T. K. Baker and M.A. Vannice, *J. Catal.,*1997, **171**, 406–419.

S7 S. Sitthisa, T. Sooknoi, Y. Ma, P.B. Balbuena, D.E. Resasco, *J. Catal.*,2011, 277, 1–13.

S8 S. Srivastava, N. Solanki, P. Mohanty, K.A. Shah, J. K. Parikh and A.K. Dalai, *Catal. Lett.,*2015, **145**, 816–823.

S9 S.H. Pang, C.A. Schoenbaum, D. K. Schwartz and J.W. Medlin, *ACS Catal.*, 2014, **4**, 3123–3131.

S10 Z. Yuan, B. Liu, P. Zhou, Z. Zhang and Q. Chi, *Catal. Sci. Technol.,* 2018, **8**, 4430–4439.

S11 J. Nie and H. Liu, *J. Catal.*,2014, **316**, 57–66.

S12 C. Carlini, P. Patrono, A.M.R. Galletti, G. Sbrana and V. Zima, *Appl. Catal. A Gen.*,2005, **289**, 197–204.

S13 Z.-Z. Yang, J. Deng, T. Pan, Q.-X. Guo and Y. Fu, *Green Chem.*, 2012, **14**, 2986–2989.

S14 P. Kisszekelyi, R. Hardian, H. Vovusha, B. Chen, X. Zeng, U. Schwingenschlögl, J. Kupai and G. Szekely, *ChemSusChem*, 2020, **13**, 3127–3136.

S15 S. Biswas, B. Dutta, A. Mannodi-Kanakkithodi, R. Clarke, W. Song, R. Ramprasad and S.L. Suib, *Chem. Commun.*, 2017, **53**, 11751–11754.